Energy Scales in the Local Magnetic Excitation Spectrum of $YBa_2Cu_3O_{6+y}$

Jan Brinckmann[1] **and Patrick A. Lee**[2]

[1] *Institut für Theorie der Kondensierten Materie, Universität Karlsruhe, D-76128 Karlsruhe, Germany*
[2] *Department of Physics, Massachusetts Institute of Technology, Cambridge, Massachusetts 02139*

The wave-vector integrated dynamical spin susceptibility $\chi_{2D}(\omega)$ of $YBa_2Cu_3O_{6+y}$ cuprates is considered. χ_{2D} is calculated in the superconducting state from a renormalized mean-field theory of the t–t'–J-model, based on the slave-boson formulation. Besides the well-known "41 meV resonance" a second, much broader peak ('hump') appears in $\mathrm{Im}\chi_{2D}$. It is caused by particle–hole excitations across the maximum gap Δ^0. In contrast to the resonance, which moves to lower energies when the hole filling is reduced from optimal doping, the position of this 'hump' at $\approx 2\Delta^0$ stays almost unchanged. The results are in reasonable agreement with inelastic neutron-scattering experiments.

PACS numbers: 71.10.Fd, 74.25.Ha, 74.72.Bk, 75.20.Hr

1. INTRODUCTION

The most prominent feature in the magnetic excitation spectrum of $YBa_2Cu_3O_{6+y}$ (YBCO) and $Bi_2Sr_2CaCu_2O_{8+\delta}$ (BSCCO) cuprates is the so-called "41 meV resonance"[1,2,3,4,5,6] at the antiferromagnetic (AF) wave vector $\mathbf{q} = (\pi, \pi)$. Its energy ω_{res} is $\approx 40\,\mathrm{meV}$ in optimally doped samples and decreases with underdoping[7,8,9,10] down to $\omega_{res} \approx 24\,\mathrm{meV}$. Recently the magnetic response has also been studied by averaging the neutron-scattering data over the in-plane 2D Brillouin zone[9,11]. The resulting local magnetic excitation spectrum $\mathrm{Im}\chi_{2D}(\omega)$ shows the above-mentioned resonance and a second, hump-like feature at an energy ω_{hump} above ω_{res}. In contrast to ω_{res}, ω_{hump} depends only weakly on the doping level. Within the calculation

to be presented in the following the 'hump' is naturally explained by particle–hole (ph) excitations across the maximum d-wave gap Δ^0. The energy $\omega_{hump} \sim 2\Delta^0$ comes out almost independent of doping. The resonance, on the other hand, emerges from a ph-bound state in the magnetic (spin-flip) channel and shows a strong doping dependence.

2. MODEL AND MEAN-FIELD THEORY

Our starting point is the doped Mott insulator. We study the t–J-model on a simple square lattice of Cu-3d orbitals for each of the two coupled CuO_2 layers (planes) in YBCO or BSCCO:

$$H = -\sum_{\nu,\nu',\sigma} t_{\nu\nu'} \widetilde{c}^{\dagger}_{\nu\sigma} \widetilde{c}_{\nu'\sigma} + \frac{1}{2} \sum_{\nu,\nu'} J_{\nu\nu'} \vec{S}_{\nu} \vec{S}_{\nu'} \ . \tag{1}$$

In the subspace with no doubly occupied orbitals, the electron operator on a Cu-lattice site ν is denoted $\widetilde{c}_{\nu\sigma}$ with spin index $\sigma = \pm 1$; $\vec{S}_{\nu}$ is the spin-density operator. A Cu-site is specified through $\nu \equiv [i,l]$, where $i = 1 \dots N_L$ indicates the Cu-position within one CuO_2-plane and $l = 1,2$ selects the layer. $t_{\nu\nu'}$ denotes the effective intra- and inter-layer Cu–Cu-hopping matrix elements, and $J_{\nu\nu'}$ the antiferromagnetic super exchange . To deal with the constraint of no double occupancy, the standard auxiliary-particle formulation $\widetilde{c}_{\nu\sigma} = b^{\dagger}_{\nu} f_{\nu\sigma}$ is used. The fermion $f^{\dagger}_{\nu\sigma}$ creates a singly occupied site (with spin σ), the "slave" boson $b^{\dagger}_{\nu}$ an empty one out of the (unphysical) vacuum $b_{\nu}|0\rangle = f_{\nu\sigma}|0\rangle = 0$. The constraint now takes the form $Q_{\nu} = b^{\dagger}_{\nu} b_{\nu} + \sum_{\sigma} f^{\dagger}_{\nu\sigma} f_{\nu\sigma} = 1$. In mean-field theory the constraint is relaxed to its thermal average $\langle Q_{\nu} \rangle = 1$. Together with the number x of doped holes per Cu-site, it fixes the fermion and boson densities to

$$(1-x) = \sum_{\sigma} \langle f^{\dagger}_{\nu\sigma} f_{\nu\sigma} \rangle \ , \quad x = \langle b^{\dagger}_{\nu} b_{\nu} \rangle \ . \tag{2}$$

The derivation of mean-field equations is presented in Ref. 12. The dynamical spin susceptibility is given in units of $(g\mu_B)^2$ as

$$\chi(\mathbf{q}, q_z, \omega) = \chi^{+}(\mathbf{q}, \omega) \cos^2(\frac{d}{2} q_z) + \chi^{-}(\mathbf{q}, \omega) \sin^2(\frac{d}{2} q_z) \ ,$$

where $\mathbf{q}$ is the in-plane wave vector, d denotes the distance of CuO_2 planes within a double-layer sandwich. For the even (+) and odd (−) mode susceptibilities a RPA-type expression is obtained,

$$\chi^{\pm}(\mathbf{q}, \omega) = \frac{\chi^{irr}_{p}(\omega)}{1 + \widetilde{J}^{\pm}(\mathbf{q}) \chi^{irr}_{p}(\omega)} \tag{3}$$

The irreducible part χ^{irr} consists of a particle–hole (ph) bubble of fermions as is known from BCS theory,

$$\chi_p^{irr}(\omega) = \frac{1}{2N_L} \sum_{\mathbf{k},\tilde{p}_z} \sum_{s,s'=\pm 1} \frac{1}{8} \left[1 + ss' \frac{\varepsilon\varepsilon' + \Delta\Delta'}{EE'} \right] \frac{f(s'E') - f(sE)}{\omega + sE - s'E' + i0_+} \tag{4}$$

with $p \equiv (\mathbf{q}, p_z)$ and $p_z = \{0, \pi\}$ for the modes $\{+,-\}$. Boson excitations do not enter χ on mean-field level. Fermions obey an effective dispersion $\varepsilon \equiv \varepsilon(\mathbf{k}, \tilde{p}_z)$, $\varepsilon' \equiv \varepsilon(\mathbf{k}+\mathbf{q}, \tilde{p}_z + p_z)$,

$$\varepsilon(\mathbf{k}, \tilde{p}_z) = -2\tilde{t}[\cos(k_x) + \cos(k_y)] - 4\tilde{t}' \cos(k_x)\cos(k_y) - \tilde{t}^{\perp}(\mathbf{k}) e^{i\tilde{p}_z}$$

and d-wave gap function $\Delta \equiv \Delta(\mathbf{k}, \tilde{p}_z)$, $\Delta' \equiv \Delta(\mathbf{k}+\mathbf{q}, \tilde{p}_z + p_z)$,

$$\Delta(\mathbf{k}, \tilde{p}_z) = \frac{\Delta^0}{2}[\cos(k_x) - \cos(k_y)] + \Delta^{\perp 0} e^{i\tilde{p}_z}$$

These enter the usual quasi-particle energy $E = \sqrt{\varepsilon^2 + \Delta^2}$, $E' = \sqrt{\varepsilon'^2 + \Delta'^2}$. Formally, vertex corrections to the simple bubble Eq. (4) have to be taken into account. However, these have almost no effect in the energy-range below $2\Delta^0$ and are therefore ignored in the following[13].

From Feynman's variation principle the effective hopping parameters are determined as[12] $\tilde{t} \approx x\,t + 0.15J$, $\tilde{t}' = x\,t'$, $\tilde{t}^{\perp}(\mathbf{k}) \approx x\,t^{\perp}(\mathbf{k})$. For the bare nearest and next-nearest neighbor hopping we assume $t = 2J$, $t' = -0.45t$, and for the inter-plane hopping[14,15] $t^{\perp}(\mathbf{k}) = 2t^{\perp}[\cos(k_x) - \cos(k_y)]^2 + t_0^{\perp}$ with $t^{\perp} = 0.1t$ and $t_0^{\perp} = 0$. We assume an in-plane superconducting order parameter Δ^0 with equal amplitude and phase in both layers. The self-consistent solution of the mean-field equations then leads to a vanishing inter-plane gap $\Delta^{\perp 0} = 0$.

Magnetic excitations in the superconducting phase are described by quasi particles (the fermions) in a BCS-type d-wave pairing state. These propagate with effective hopping parameters $\tilde{t}$, $\tilde{t}'$ strongly reduced from the bare parameters t, t' by the small Gutzwiller factor x. The bubble Eq. (4) describes spin-flip ph-excitations of these particles, which are subject to the mode-dependent final-state interaction in Eq. (3),

$$\tilde{J}^{\pm}(\mathbf{q}) = \alpha J(\mathbf{q}) \pm J^{\perp}\ ,\ J(\mathbf{q}) = 2J[\cos(q_x) + \cos(q_y)] \tag{5}$$

The inter-plane exchange is chosen as $J^{\perp} = 0.2J$. The destruction of the antiferromagnetic (AF) state of the 1/2-filled system by hole doping[16,17,18,19] is missing in mean-field theory. The necessary correlations of fermions and bosons are not contained, and the AF order vanishes at an unphysically high doping level[20] $x_c^0 \approx 0.22$. Therefore we assume[12,21] a renormalization

$J \to \alpha J$ of the in-plane nearest–neighbor exchange. Using $\alpha = 0.35$ reduces x_c^0 down to $x_c \approx 0.03$, which is consistent with experiment and makes the study of underdoped systems possible. Note that the above-mentioned renormalization $t \to \widetilde{t}$ of the quasi-particles comes out of the self-consistent calculation, whereas $J \to \alpha J$ is a phenomenological model. Our assumption of α being independent of doping leads to an AF correlation length[12] $\xi_{AF}(x) \sim 1/\sqrt{x - x_c}$ at $T \to 0$, which agrees with known experimental[22] and theoretical[23] results.

3. RESULTS

From the susceptibility Eq. (3) the local magnetic excitation spectrum is determined from

$$\mathrm{Im}\chi^{\pm}_{2D}(\omega) = \iint_{-\pi}^{\pi} \frac{\mathrm{d}^2 q}{(2\pi)^2}\, \mathrm{Im}\chi^{\pm}(\mathbf{q}, \omega) \tag{6}$$

Fig. 1 shows $\mathrm{Im}\chi_{2D}$ for the odd and even mode at $T \to 0$ in the superconducting state. A resonance is clearly visible in the odd $(-)$ mode, at an energy $\omega_{res} = 0.42J \approx 50\,\mathrm{meV}$ for $x = 0.12$ near optimal doping. When x is reduced (underdoping) the resonance moves to lower energies and gains spectral weight. The resonance appears at the same energy[12] as in $\mathrm{Im}\chi^{-}(\mathbf{q}, \omega)$ for fixed wave vector $\mathbf{q} = (\pi, \pi)$. In addition, both modes $\mathrm{Im}\chi^{\pm}_{2D}(\omega)$ show a broad peak ('hump') at energies $\omega^{-}_{hump} \approx \omega^{+}_{hump}$ above ω_{res}. In contrast to ω_{res} the hump-maxima $\omega^{\pm}_{hump}$ are almost independent of doping, located somewhat below $2\Delta^0$ ($2\Delta^0 \approx 0.7J$ for $x = 0.12$).

The resonance emerges from a pole in Eq. (3) at wave-vector (π, π) and energy ω_{res}, driven by the effective interaction Eq. (5) in the odd $(-)$ mode. Since ω_{res} is slightly below the threshold Ω_0 to the particle–hole (ph) continuum, the resonance appears undamped, i.e., as a δ-function. Due to the inter-layer coupling $J^{\perp}$ the interaction Eq. (5) is weaker in the even $(+)$ mode, and the resonance in $\mathrm{Im}\chi^{+}$ is shifted up into the ph-continuum, becoming almost suppressed. Consequently, in wave-vector space a sharp peak around (π, π) is visible only in the odd $(-)$ mode. This is demonstrated in the top panel of Fig. 2. The bottom panel of that figure shows the magnetic response at a higher energy close to the hump-maxima $\omega^{\pm}_{hump}$. The intensity is much reduced compared to the resonance. However, the magnetic excitations at $\approx \omega_{hump}$ occupy almost the whole 2D Brillouin zone, and despite their small amplitude they contribute to the wave vector integrated susceptibility Eq. (6). The 'hump' can be traced back to ph-excitations across the maximum gap Δ^0: At $\mathbf{q} = (\pi, \pi)$ the irreducible particle–hole

Local Magnetic Excitation Spectrum of $YBa_2Cu_3O_{6+y}$

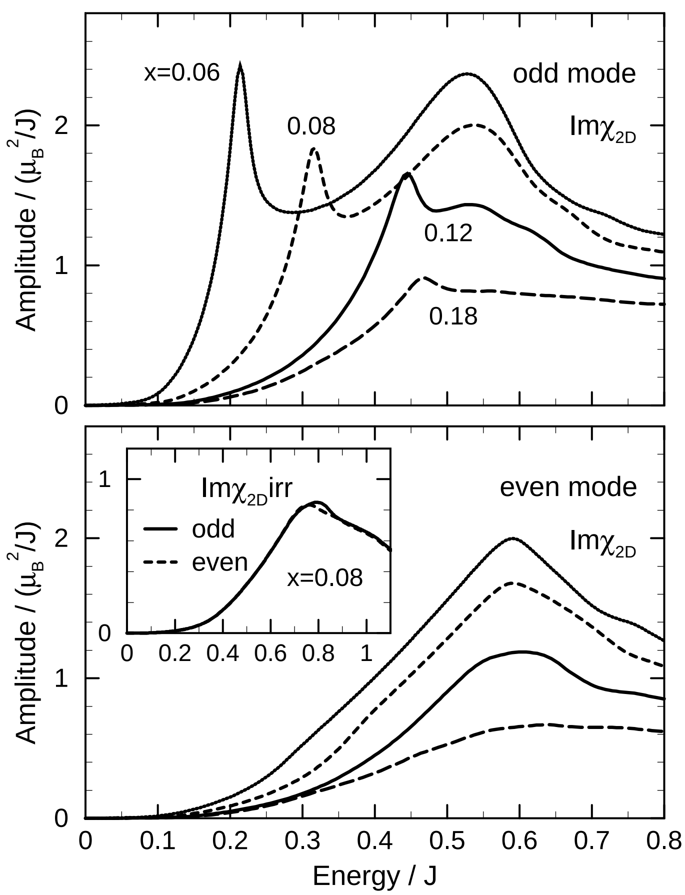

Fig. 1. Wave-vector **q** integrated odd- and even-mode susceptibilities $\mathrm{Im}\chi_{2D}$ for hole filling $x = 0.06 \ldots 0.18$. Parameters are $t = 2J$, $t' = -0.45t$, $t^{\perp} = 0.1t$, $J^{\perp} = 0.2J$. Curves are calculated with a damping FWHM= $0.04J \approx 5\,\mathrm{meV}$. **Inset: q**-integrated bubble spectrum $\mathrm{Im}\chi_{2D}^{irr}$ for $x = 0.08$. The maximum is located close to $2\Delta^0 = 0.78J$.

bubble $\mathrm{Im}\chi^{irr}(\mathbf{q}, \omega)$ shows a log-type van Hove singularity (vHs) at $\omega = 2\Delta^0$, remnant of the density of states of the d-wave superconductor. Moving off (π, π) this vHs splits into three vHs that disperse very weakly throughout the Brillouin zone, leading to a soft maximum ('hump') at $2\Delta^0$ in the **q**-integrated (local) bubble spectrum $\mathrm{Im}\chi_{2D}^{irr}(\omega)$. This is shown in the inset of Fig. 1. When the final-state interaction Eq. (5) is taken into account, the resonance is obtained in the odd mode, and the hump is pulled down to $\omega_{hump}^{-} < \omega_{hump}^{+} < 2\Delta^0$. Also is the doping dependence of Δ^0 compensated: $\omega_{hump}^{\pm}$ are independent of doping, while Δ^0 increases with underdoping.

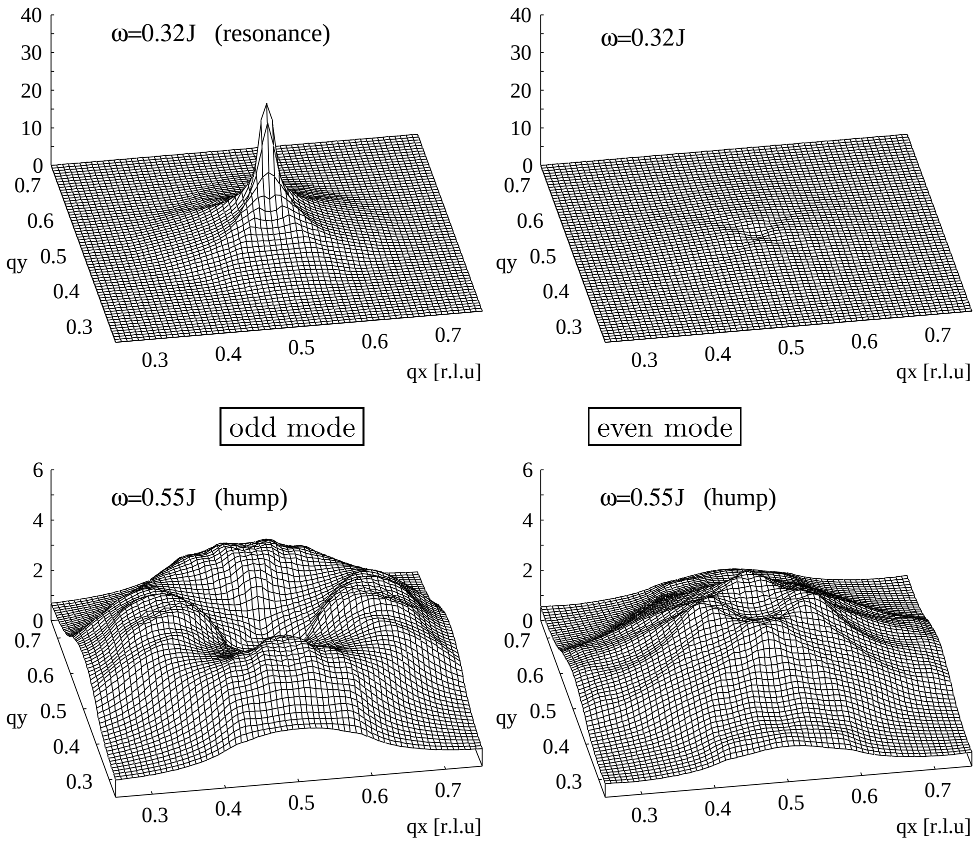

Fig. 2. Magnetic response $\mathrm{Im}\chi^{(\pm)}$ (in arbitrary units) in wave-vector $\mathbf{q}$ space for $x = 0.08$. q_x, q_y are measured in units of $2\pi = 1$r.l.u. Parameters as in Fig. 1. **Top:** At the energy $\omega = \omega_{res}$ where the resonance appears in the odd mode. **Bottom:** At an energy ω close to the 'hump'-maxima in both modes. (Note the different amplitude scale.)

4. COMPARISON TO EXPERIMENT

Two experimental groups studied the wave-vector integrated magnetic response $\mathrm{Im}\chi^{\pm}_{2D}$ in underdoped YBCO. Refs. 11,24 reported a line shape for $\mathrm{YBCO}_{6.6}$, which agrees quite well with our theoretical result for $x \leq 0.08$. A 'hump' in $\mathrm{Im}\chi^{+}_{2D}$ (even) appears at $\approx 100\,\mathrm{meV}$, $\mathrm{Im}\chi^{-}_{2D}$ (odd) shows a similar structure at a somewhat lower energy $\approx 90\,\mathrm{meV}$. The well-known resonance appears only in $\mathrm{Im}\chi^{-}_{2D}$ at $34\,\mathrm{meV}$. In Refs. 9,25 two underdoped samples $\mathrm{YBCO}_{6.7}$ and $\mathrm{YBCO}_{6.5}$ have been studied. In the even ("optical") mode of $\mathrm{YBCO}_{6.7}$ a hump appears around $70\,\mathrm{meV}$, whereas the odd ("acoustic")

mode shows a weak hump-like structure at $\approx 55\,\mathrm{meV}$, separated from the resonance at $33\,\mathrm{meV}$. These features tend to move up in energy in the more underdoped sample $\mathrm{YBCO}_{6.5}$, while the resonance in $\mathrm{Im}\chi^{-}_{2D}$ shifts down to $25\,\mathrm{meV}$.

Although the detailed experimental line shapes are not unique, the qualitative features of our calculation are found in the neutron-scattering spectra. In particular we reproduce the different dependencies on doping level of the resonance at ω_{res} in the odd mode and the hump-like feature at $\omega^{\pm}_{hump}$ in both modes. Also is ω^{-}_{hump} of the odd mode lower than the ω^{+}_{hump} of the even mode. Theory and experiments can also be compared quantitatively. The measured neutron-scattering intensities[9,11] are of the same order as the theoretical ones in Fig. 1 (using $J = 120\,\mathrm{meV}$, i.e., $1\mu_B^2/J = 8.3\mu_B^2/\mathrm{eV}$). The maximum of the hump in the even, odd mode in Fig. 1 occurs at $\omega^{+,-} \approx 0.6J, 0.53J = 72\,\mathrm{meV},\ 64\,\mathrm{meV}$, in good agreement with the measurements Ref. 9 on $\mathrm{YBCO}_{6.7}$ at low temperature.

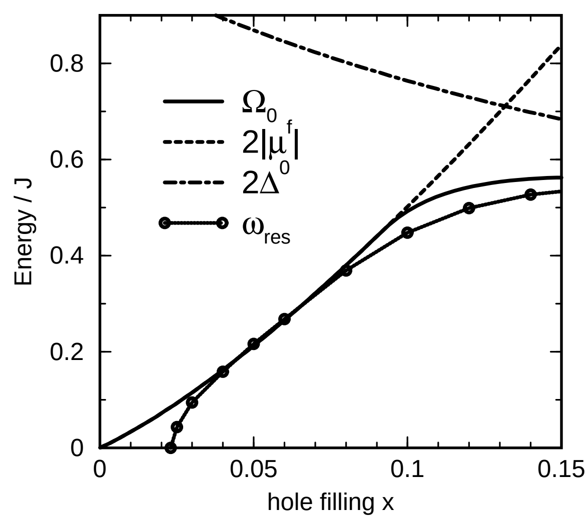

Fig. 3. $2|\mu^f|$, $2\Delta^0$, the ph-threshold Ω_0, and the resonance energy ω_{res} as function of doping at $T \to 0$.

5. CONCLUSION

The local magnetic excitation spectrum $\mathrm{Im}\chi^{\pm}_{2D}(\omega)$ is characterized by two energy scales that behave differently with hole filling x (doping). The

resonance energy ω_{res} follows the particle–hole threshold Ω_0, which in underdoped systems is determined by the chemical potential μ^f of the fermions as $\omega_{res} \leq \Omega_0 = 2|\mu^f|$. The maxima of the humps, on the other hand, are determined by the gap Δ^0 through $\omega^{\pm}_{hump} \sim 2\Delta^0$. When x is reduced from optimal doping, $|\mu^f|$ and therefore ω_{res} decrease quickly, while Δ^0 increases. This is displayed in Fig. 3. It has been noted above that the mean-field theory describes magnetic excitations in terms of quasi particles (QP) (the fermions) with a reduced Fermi velocity $\widetilde{v}_F \approx (x + 0.15J/t)\, v_F$. Hence in underdoped systems the QP's chemical potential comes out (much) smaller than the gap, $|\mu^f| < \Delta^0$, and thus determines the scale for ω_{res}. This leads to the observed decoupling of the resonance energy from the gap Δ^0, while Δ^0 is still visible through the 'humps' in the local spectrum $\mathrm{Im}\chi^{\pm}_{2D}$.

ACKNOWLEDGMENTS

This work has been supported by the Deutsche Forschungsgemeinschaft through SFB 195 and the NSF under MRSEC Program No. DMR 98-08941.

REFERENCES

1. J. Rossat-Mignod *et al.*, Physica B **169**, 58 (1991).
2. H. A. Mook *et al.*, Phys. Rev. Lett. **70**, 3490 (1993).
3. H. F. Fong *et al.*, Phys. Rev. Lett. **75**, 316 (1995).
4. P. Bourges, L. P. Regnault, L. Sidis, and C. Vettier, Phys. Rev. B **53**, 876 (1996).
5. H. He *et al.*, Phys. Rev. Lett. **86**, 1610 (2001).
6. J. Mesot *et al.*, (2001), preprint cond-mat/0102339.
7. P. Dai *et al.*, Phys. Rev. Lett. **77**, 5425 (1996).
8. H. F. Fong, B. Keimer, D. L. Milius, and I. A. Aksay, Phys. Rev. Lett. **78**, 713 (1997).
9. H. F. Fong *et al.*, Phys. Rev. B **61**, 14773 (2000).
10. P. Dai, H. A. Mook, R. D. Hunt, and F. Doğan, Phys. Rev. B **63**, 054525 (2001).
11. P. Dai *et al.*, Science **284**, 1344 (1999).
12. J. Brinckmann and P. A. Lee, (2001), preprint cond-mat/0107138.
13. J. Brinckmann and P. A. Lee, J. Phys. Chem. Solids **59**, 1811 (1998).
14. S. Chakravarty, A. Sudbø, P. W. Anderson, and S. Strong, Science **261**, 337 (1993).
15. O. K. Andersen, O. Jepsen, A. I. Lichtenstein, and I. I. Mazin, Phys. Rev. B **49**, 4145 (1994).
16. T. K. Lee and S.-P. Feng, Phys. Rev. B **38**, 11809 (1988).
17. J. Igarashi and P. Fulde, Phys. Rev. B **45**, 12357 (1992).

18. G. Khaliullin and P. Horsch, Phys. Rev. B **47**, 463 (1993).
19. D. H. Kim and P. A. Lee, Ann. Phys. (N.Y.) **272**, 130 (1999).
20. M. Inaba, H. Matsukawa, M. Saitoh, and H. Fukuyama, Physica C **257**, 299 (1996).
21. J. Brinckmann and P. A. Lee, Phys. Rev. Lett. **82**, 2915 (1999).
22. T. R. Thurston *et al.*, Phys. Rev. B **40**, 4585 (1989).
23. R. R. P. Singh and R. L. Glenister, Phys. Rev. B **46**, 11871 (1992).
24. S. M. Hayden *et al.*, Physica B **241–243**, 765 (1998).
25. P. Bourges *et al.*, Phys. Rev. B **56**, R11439 (1997).